Sensitivity to S-Cone Stimuli and the Development of Myopia

Christopher Patrick Taylor,[1] Timothy G. Shepard,[2] Frances J. Rucker,[1] and Rhea T. Eskew Jr[2]

[1]New England College of Optometry, Boston, Massachusetts, United States
[2]Psychology, Northeastern University, Boston, Massachusetts, United States

Correspondence: Christopher Patrick Taylor, Department of Biomedical Science and Disease, New England College of Optometry, 424 Beacon Street, Boston, MA 02115, USA;
taylorc@neco.edu.

CPT and TGS contributed equally to the work presented here and should therefore be regarded as equivalent authors.

Submitted: February 14, 2018
Accepted: August 8, 2018

Citation: Taylor CP, Shepard TG, Rucker FJ, Eskew RT Jr. Sensitivity to S-cone stimuli and the development of myopia. *Invest Ophthalmol Vis Sci*. 2018;59:4622–4630. https://doi.org/10.1167/iovs.18-24113

Purpose. Longitudinal chromatic aberration (LCA) is a color signal available to the emmetropization process that causes greater myopic defocus of short wavelengths than long wavelengths. We measured individual differences in chromatic sensitivity to explore the role LCA may play in the development of refractive error.

Methods. Forty-four observers were tested psychophysically after passing color screening tests and a questionnaire for visual defects. Refraction was measured and only subjects with myopia or hyperopia without severe astigmatism participated. Psychophysical detection thresholds for 3 cyc/deg achromatic, L-, M-, and S-cone–isolating Gabor patches and low-frequency S-cone increment (S+) and decrement (S−) blobs were measured. Parametric Pearson correlations for refractive error versus threshold were calculated and nonparametric bootstrap 95% percentage confidence intervals (BCIs) for r were computed.

Results. S-cone Gabor detection thresholds were higher than achromatic, L-, and M-cone Gabors. S-cone Gabor thresholds were higher than either S+ or S− blobs. These results are consistent with studies using smaller samples of practiced observers. None of the thresholds for the Gabor stimuli were correlated with refractive error (RE). A negative correlation with RE was observed for both S+ ($r = -0.28$; $P = 0.06$; BCI: $r = -0.5$, -0.04) and S− ($r = -0.23$; $P = 0.13$; BCI $= -0.46$, 0.01) blobs, although this relationship did not reach conventional statistical significance.

Conclusions. Thresholds for S+ and S− stimuli were negatively related to RE, indicating that myopes may have reduced sensitivity to low spatial frequency S-cone stimuli. This reduced S-cone sensitivity might have played a role in their failure to emmetropize normally.

Keywords: myopia, color, detection, S-cone

Myopia usually occurs when the eye is too long for its optics. Myopia is often considered a minor visual defect, but myopia increases the relative risk of eye disease to an extent equal or greater than smoking does for the development of cardiovascular disease.[1] The prevalence and associated costs of care for myopia and myopia-related ocular disorders are substantial, estimated to be in the billions of dollars in the United States and worldwide.[2–4] Thus, even small advances in the understanding of the development and control of myopia could lead to meaningful benefits for public health.

Emmetropization refers to the process that alters the eye's growth rate after birth in order to bring the size of the eye in line with the focal power. The stimulus factors that guide emmetropization are of great interest to the myopia research community.[5] One possible factor that might assist in emmetropization is longitudinal chromatic aberration (LCA), the shift in the focal plane that varies with wavelength.[6–8] Short-wavelength (blue) light has a shorter focal length than long-wavelength (red) light. This change in focal plane generates blur, which indicates the sign of defocus. The effect of LCA on the retinal image is quite large (approximately 3 diopters [D] of blur over the visible spectrum; see Chapter 17 in Atchison and Smith[9]). Although there are individual differences in measured LCA[9] these differences are relatively small; however, individuals may differ in the effect that chromatic blur has on emmetropization because this effect depends on processes beyond the optics of the eye.

Evidence for the use of LCA to guide emmetropization can be found in the chick model,[10–12] a fundamental model for the understanding of ocular disease and emmetropization.[13,14] An advantage of the chick model, over other animal models of myopia, arises from the chick visual system, which can encode a rich array of color signals.[15] This benefit of the chick model has borne fruit experimentally. Chicks reared under broad spectrum illuminants show remarkable changes in growth depending on whether the blue light component of white light is present or absent; the presence of blue light in the illuminant slows the increase in growth produced by low (0.2 Hz) temporal frequency flicker,[16,17] suggesting that short-wavelength light provides a protective signal to stop or slow the emmetropization process. Converging evidence in the literature points to a role for blue light in the emmetropization process in a variety of species[10,11,18–20] including humans.[21,22]

In the chick model, short-wavelength (S) cone signals can alter the response to lens-induced defocus.[12] The emmetropization system of the chick compensates for lens-induced wavelength defocus when it is stimulated with dim (0.67 lux) blue monochromatic light by altering the rate of eye growth.[12] In this experiment, the short-wavelength light intensity is low enough that the stimulation of the other cone types is below

the level at which they could contribute to emmetropization, indicating that the effect of blue light is due to S-cone responses.[23] Further bolstering the case that LCA can provide the sign of defocus to the emmetropizing chick, it has been shown that the chick emmetropization system can infer a signed chromatic signal when presented with spatial sine-wave patterns that simulate hyperopic (blue contrast higher than red) and myopic defocus (red contrast higher than blue).[6]

If LCA contributes to emmetropization in chickens, then S-cones may be involved in human emmetropization. The human short-, medium-, and long-wavelength cones (i.e., S-, M-, and L-cones) have peak fundamentals at about 442, 542, and 570 nm, respectively.[24,25] Thus, LCA could produce a larger dioptric difference signal between S-cones and the other cone types, compared to any difference between L- and M-cones, and it is therefore likely that any contribution of LCA to emmetropization will occur via S-cone signals. S-cone signals can alter accommodation in humans.[26–28] Given that near-work has been shown to be a contributing factor to the development of myopia,[5,29] it is possible that the S-cone influence on accommodation may contribute to either the success or failure of emmetropization.

Sensitivity to color signals, mediated by the three cone types, could be differentially affected by numerous factors, most of which have been shown to differ among individuals.[30] These include differences in photopigment λ_{max},[31] preretinal filtering (primarily by the lens and macular pigment),[32] cone density and packing arrangement,[33,34] and the effects of different spatial and temporal characteristics of the stimuli (via the characteristically different neural pathways underlying psychophysically defined mechanisms)[35,36]; for a review, see Reference 37.

Some of these factors might be expected to have effects that persist over the adult lifetime of the individual, such as the relative numbers and spatial distribution of L-, M-, and S-cones in the retinal mosaic, while others could vary with age and other factors.[37] We hypothesize that LCA could play the same role in human emmetropization as in the chick model. During development, individual differences in cone contrast sensitivity may contribute to differences in the efficacy of the emmetropization mechanisms. If individual differences in L-, M-, and S-cone contrast sensitivity persist from the early sensitive period for emmetropization into adulthood, then we expect there to be a correlation between psychophysically determined chromatic detection thresholds and refractive error, especially for S-cone–isolating test stimuli.

Methods

Observers

A total of 44 adult observers participated in the experiment. The mean age was 25.8 years and standard deviation, 5.6 years. All but three observers were between 20 and 29 years of age; three observers outside this range were 35, 39, and 54 years. There were 13 male and 31 female observers. Ten of the observers were Asian and the rest Caucasian. Before the experiment, observers were given a health and medical questionnaire. Observers were only included in the study if they had no systemic disease, ocular abnormalities, a central astigmatism of less than 1.75 D, anisometropia of less than 1.0 D, no history of othokeratology or corneal refractive surgery, no fixational instability or restricted eye movement, no history of ocular pathology, and no ocular medications. Each observer's refraction was measured with an autorefractor (Grand Seiko model WR-5100K; Shigya Machinery Works, Hiroshima, Japan) and confirmed with subjective refraction to ensure that visual acuity was corrected to normal for the experiment.

A Nagel anomaloscope and a Farnsworth-Munsell 100 Hue color vision test, given under illumination by a Macbeth daylight lamp, were used to screen for color vision anomalies.[38] All observers scored within the normal range.

The research protocol was approved by the New England College of Optometry and the Northeastern University Institutional Review Boards; observers gave informed consent at both institutions. The procedures complied with the Declaration of Helsinki.

Apparatus

A G3 Power Macintosh computer with an ATI Radeon 7500 video board (Apple, Cupertino, CA, USA), with a driver verified to support the 10-bit digital-to-analog converters, was used to display the stimuli, using custom software. The display was a SONY GDMF520 CRT monitor (Sony, Tokyo, Japan) set to a refresh rate of 75 Hz.

A mean gray background field, which was present throughout the experiment, had CIE coordinates $x = 0.306$, $y = 0.309$, and a luminance of 70 cd/m^2. Spectroradiometric characterization was performed at 4 nm intervals across the spectrum by using a Photo Research PR-650 spectroradiometer (Photo Research, Syracuse, NY, USA). The luminance nonlinearity of the display was corrected with gamma correction lookup tables.

Head position was stabilized with a chin and forehead rest. Viewing distance was 52 cm from the pupil. Spherical and cylindrical corrections were made by using trial lenses mounted 13 mm in front of the preferred eye. For the correlational analyses described in Results, refractive error is given as "best sphere" (or spherical equivalent), which is the spherical power plus half the cylindrical power. The LCA produced by the trial lenses was calculated to be negligible (for our most myopic observer, the effect was 0.15 D of chromatic aberration with a –8 D BK7 lens material between 435 nm and 656 nm with a back-vertex distance of 13 mm).

Stimuli

Two spatial patterns were used as test stimuli. One type was an oriented Gabor patch with a spatial frequency of 3 cyc/deg and a two-dimensional Gaussian envelope ($\sigma = 2°$). The sinusoidal component of the Gabors (in sine phase relative to the center of the screen) was modulated along four different directions in cone contrast space: achromatic (black-white) and the three cone-isolating directions (L, M, and S). The second pattern was a two-dimensional Gaussian blurred spot (a blob) with a center spatial frequency of ≈ 0 cyc/deg and a size-constant of $\sigma = 2°$. Blobs were modulated to produce either increments (S+, purplish) or decrements (S–, lime-green) in S-cone quantal catch (without modulating L- or M-cones). The blobs have the same overall size as the Gabor patch but allow increment and decrement modulations to be studied independently and are dominated by very low spatial frequencies. Examples of the stimuli are shown in Figure 1.

Test stimuli were presented against the constant gray background field. Cone-isolating stimuli were created by using standard "silent substitution" methods,[39] in which the red, green, and blue guns of the CRT display were modulated to produce changes in a single cone type. These cone-isolating color directions were calculated by cross-multiplying the measured spectra of the monitor's guns with the L-, M-, and S-cone fundamentals,[24,25] all in quantal units, and calculating the relative red, green, and blue gun modulations required to alter quantal catch rates in one cone type at a time. This

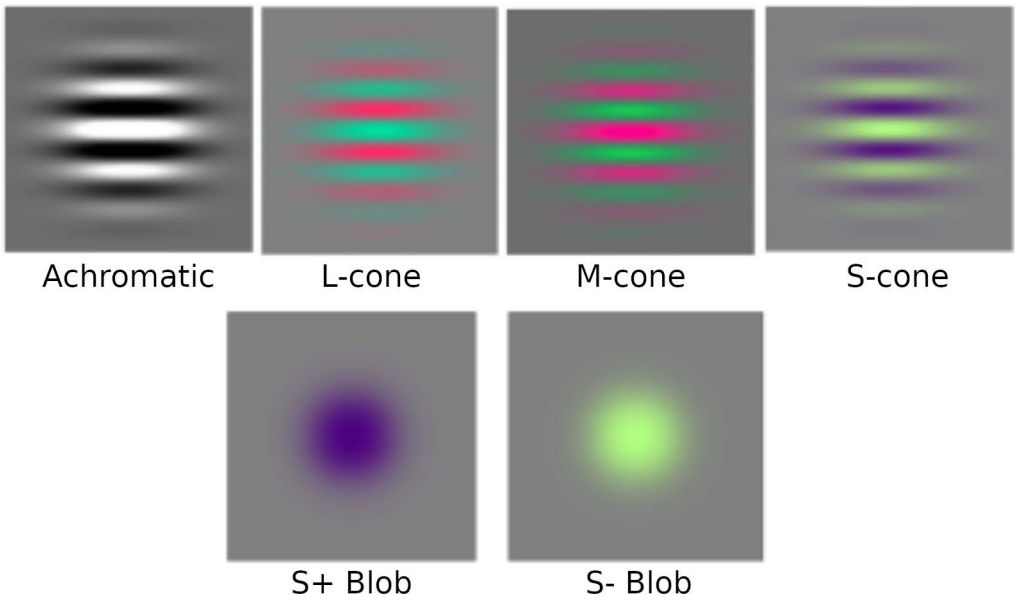

Figure 1. The *top* row shows high-contrast versions of the achromatic, L-, M-, and S-cone Gabors. The *bottom* row shows S+ increment and S– decrement blobs. The colors are only approximately correct owing to the reproduction process.

method is widely used in color vision psychophysics.[40–42] Although there are individual differences in the S-cone–isolating direction, these differences are generally thought to be minor at threshold with broad-band primary stimuli like those in a CRT monitor (e.g., see Smith and Pokorny[30]). Stimulus strength is defined in cone contrast units. For example, for the L-cone Gabor patch, cone contrast is:

$$\frac{\Delta L}{L} = \frac{L_{peak} - L_{bg}}{L_{bg}}. \quad (1)$$

The terms on the right refer to L-cone quantal catch, where L_{bg} is the background catch produced by a gray mean field. L_{peak} refers to the maximum quantal catch produced by the Gabor. M- and S-cone contrasts are defined in the same way. The achromatic contrast was defined as:

$$\sqrt{\left(\frac{\Delta L}{L}\right)^2 + \left(\frac{\Delta M}{M}\right)^2 + \left(\frac{\Delta S}{S}\right)^2}, \quad (2)$$

which is $\sqrt{3}$ times larger than Weber luminance contrast.[43] The maximum cone contrast available in our display was 0.205, 0.239, 0.874, and 1.732 for the L, M, S, and achromatic color directions. Cone contrast provides a physiologically relevant way to quantify the strength of the stimulus in terms of the modulation it produces in the cones (see Ref. 43 for review); it takes into account the overlap of the cone fundamentals and indexes the magnitude of the signals provided to postreceptoral neural mechanisms. Unlike some other potential measures of chromatic contrast, cone contrast values are independent of the particular stimulating apparatus and of the particular observer under study.

Table 1 lists CIE x and y coordinates of the peak modulations of the cone-isolating stimuli (i.e., the largest incremental and decremental cone modulations that could be produced by the apparatus). The S+ and S– blobs have the same chromaticities as the peak and trough of the S-cone Gabor patch. Both the peak and trough of the achromatic modulation have the same chromaticity as the background field (0.306, 0.309), by definition.

Temporally, the stimulus appeared on the screen abruptly and then was linearly ramped off in contrast until its contrast was reduced to zero (which occurred at 333 ms). Fixation was guided by four thin black diagonal lines, each pointing at the center of the screen, ending 1.5 from the center, which were present throughout the experiment.

Procedure

A two-interval forced choice method was used. Observers were presented with two 333-ms intervals. Each interval was marked by clearly audible tones. One interval contained the stimulus (target interval) and the other a blank (foil interval). The order of the target and foil interval was random on each trial. The target and foil intervals were temporally separated by a 400-ms interstimulus blank interval. Observers reported, via two keys on the keyboard, which interval they perceived to be the target. Auditory feedback was provided to inform the observer whether their response was correct or incorrect.

At the start of each session observers verified that the fixation stimuli looked sharp through the trial lens(es) provided. Before each block of trials the observer adapted to the gray background field for 60 seconds. Observers initiated each trial with a key press. In each block, only one type of test pattern was presented at different contrast levels. A staircase procedure[44] was used to select the test contrast on each trial.

Table 1. CIE Chromaticity Coordinates of the Ends of the Cone Vectors*

Peak	x	y
L_+	0.367	0.302
$L-$	0.222	0.320
M_+	0.232	0.355
$M-$	0.372	0.269
S_+	0.270	0.222
$S-$	0.384	0.499

* The chromaticity at the maximum contrast available in each cone-isolating direction, for the increment/positive and decrement/negative peaks.

Table 2. Descriptive Statistics for the Six Conditions in Cone Contrast Units

Stimulus	Mean	Median	Winsorized	SD	Median 95% BCI	CV
A Gabor	0.044	0.026	0.032	0.089	0.021, 0.029	2.015
L Gabor	0.017	0.013	0.015	0.016	0.011, 0.015	0.944
M Gabor	0.025	0.019	0.023	0.024	0.015, 0.022	0.960
S Gabor	0.182	0.167	0.178	0.078	0.133, 0.210	0.429
S+ blob	0.097	0.083	0.089	0.073	0.066, 0.094	0.755
S− blob	0.113	0.094	0.101	0.105	0.081, 0.105	0.928

The mean is the threshold arithmetic mean. Winsorized is the arithmetic mean of middle 95% with Winsorizing. Median 95% BCI is the confidence interval of the median determined by the the bootstrap percentile method. See the text for additional information. CV, coefficient of variation (SD/mean); SD, standard deviation.

Weibull functions were fit to the accumulated frequency-of-seeing data to estimate contrast threshold (the stimulus contrast required for 82% correct performance). Thresholds from multiple runs were averaged (3–4 runs for each participant for each stimulus type).

The experiment was run in two different sessions on two separate days. Gabor test runs of different chromaticities (L-, M-, S-, and achromatic) were block randomized for the first session, and the S+ and S− blobs were block randomized in the second session.

Results

Table 2 presents the descriptive statistics and Figure 2 the thresholds in each of the six conditions. S-cone Gabor thresholds are higher than the achromatic, L-cone, or M-cone Gabor thresholds, which is consistent with previous results.[43,45,46] Thresholds for the L- and M-Gabors are very similar while achromatic Gabor thresholds are higher.

Table 2 and Figure 2 also show that the thresholds for the S-cone Gabors are higher than both the S-cone increment (S+) or decrement (S−) thresholds. We also found that thresholds for

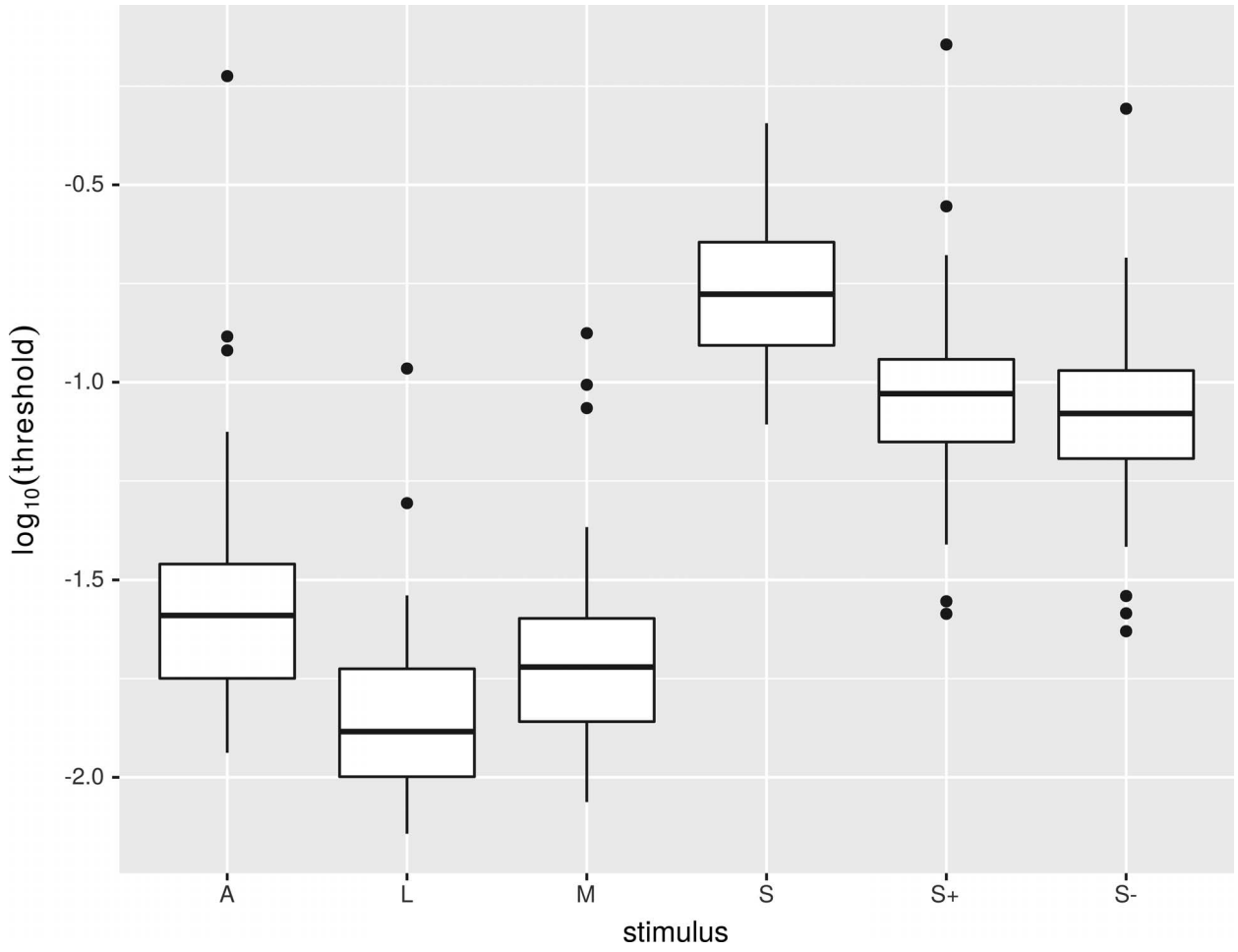

Figure 2. Box and whisker plot of $\log_{10}$(threshold), in cone contrast units, as defined in Equations 1 and 2, for the six chromatic conditions. Boxes cover the interquartile range, whiskers are 1.5 times the interquartile range, and outliers are shown as *black circles*.

Investigative Ophthalmology & Visual Science

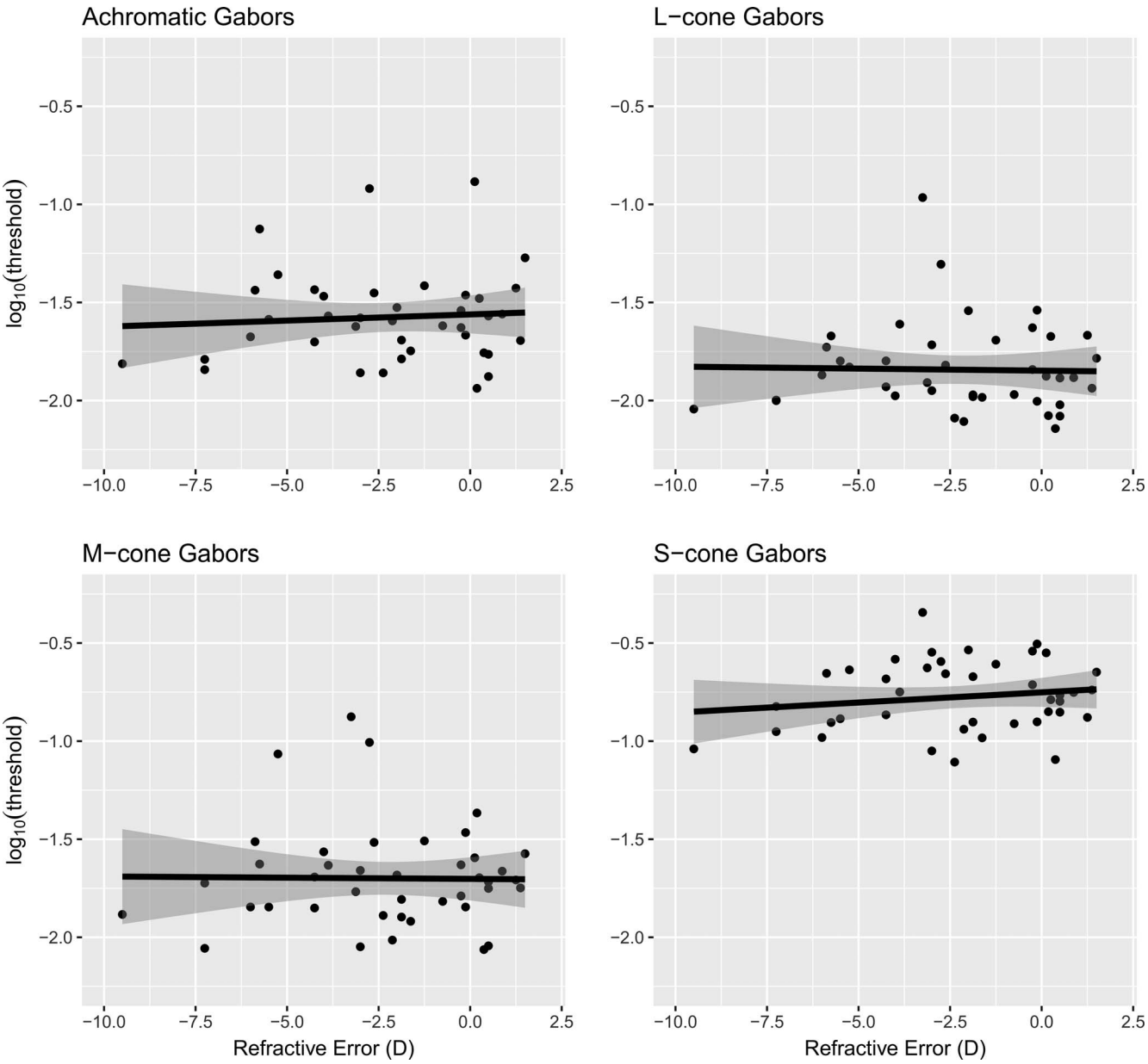

FIGURE 3. Refractive error versus $\log_{10}$(threshold) for the achromatic, L-, M-, and S-Gabor conditions. Each point is an observer's threshold, the line the best-fitting regression line, and the *gray shaded region* the 95% confidence interval of the fit (Chambers and Hastie[47]).

the S-cone increment blobs are slightly higher than for the S-cone decrement blobs.

The last three columns of Table 2 give the standard deviation, 95% bootstrap confidence interval (BCI) for the median, and coefficient of variation (standard deviation divided by the mean) of the thresholds. The BCI for the median was computed by using the bootstrap package in R[47–49] with 999 bootstrap resamples. All of our measures of variability indicate that it is substantial among our naive and/or unpracticed observers compared to what is typically seen in psychophysical detection tasks using practiced observers. Figure 3 shows scatterplots of log threshold versus refractive error (reported as best sphere) for the Gabors; Figure 4 shows the same relationship for the S-cone blobs. The best-fitting regression line and the 95% confidence region around that fit are indicated.

Table 3 gives the correlation between log threshold and refractive error for each of the stimuli. None of the Gabor detection thresholds were correlated with refractive error at an $\alpha = 0.05$ using parametric tests (even without correcting for multiple comparisons) and the BCIs include zero.

However, there were stronger relationships for the S+ and S– blob stimuli. The parametric statistical tests of the correlation coefficient for the blobs approached an uncorrected conventional $\alpha = 0.05$, but the bootstrap confidence intervals show that these relationships suggest a negative correlation, especially for the S+ blob where the 95% BCI does not include zero. Omitting the most myopic observer—leftmost points in each panel in Figure 4—causes the *P* value for S+ to be 0.047 (i.e., it reaches conventional significance) and S– to be 0.11 (i.e., to further trend toward significance). However, removing data to achieve a threshold *P* value is an example of the pernicious scientific practice known as "*P*-

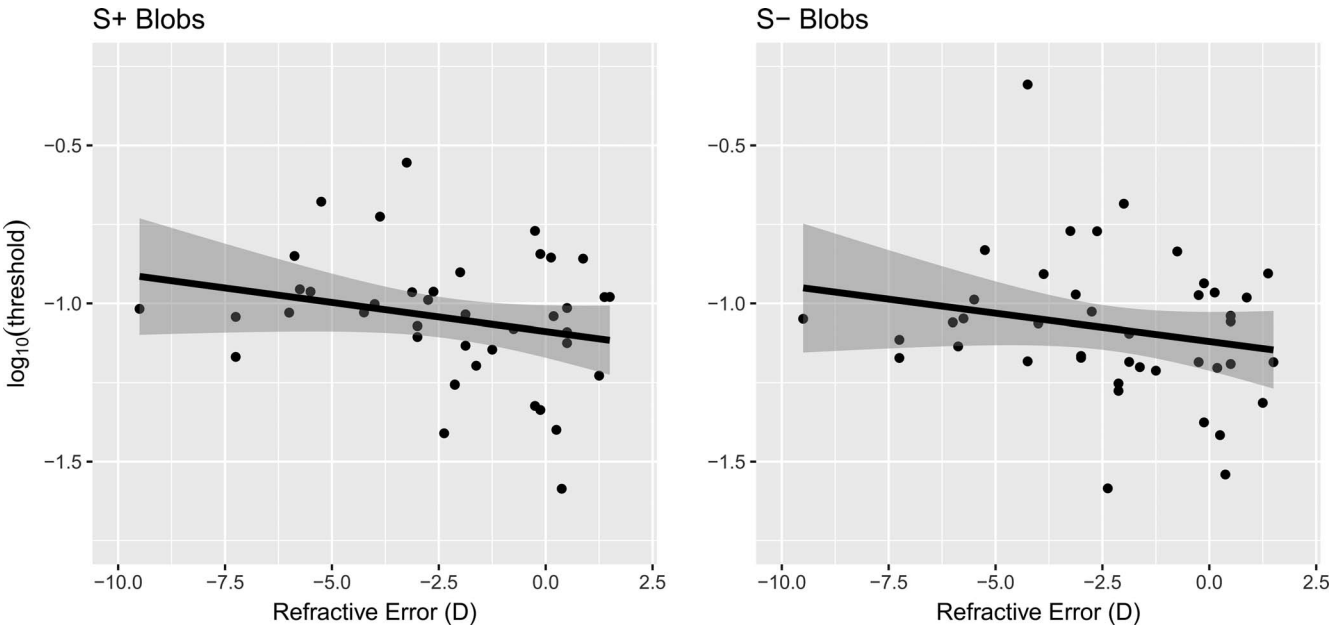

Figure 4. Refractive error (best sphere) versus threshold for the S+ increment and S− decrement blob conditions. Each point is an observer's threshold, the line the best-fitting regression line, and the *gray shaded region* the 95% confidence interval of the fit (Chambers and Hastie[47]).

hacking."[50] The bootstrap procedure provides a more principled method to protect against outliers.

Discussion

The pattern of thresholds for the different cone-isolating stimuli (Fig. 2; Table 2) is consistent with previous studies.[43,45,46] Under most circumstances, L- and M-cone contrast modulations are detected by highly sensitive chromatic neural mechanisms that use the difference of approximately equally weighted L- and M-cone signals.[40,43] Therefore, it is likely that observers detected the L- and M-cone stimuli via the L-M pathways. When thresholds are measured in cone contrast units, these "reddish-greenish" or L-M mechanisms are substantially more sensitive than either the achromatic mechanism[41] or mechanisms with appreciable S-cone inputs.[43]

S-cone Gabor and blob increment (S+) and decrement (S−) thresholds are higher than the L-, M-, and achromatic Gabor thresholds because of the reduced sensitivity of the S-cone mechanisms. Additionally, the threshold for S-cone Gabors are higher than the thresholds for the S+ and S− blobs, which may be the product of the blobs having a lower center spatial (≈ 0 cyc/deg) frequency than the 3 cyc/deg S-cone Gabor stimuli.[51,52] We observed that S-cone blob increment (S+) thresholds are slightly higher than the decrement (S−) thresholds (consistent with the studies of Wang et al.[42] and Bosten et al.[53]). The clearest result is that the association between S+ and S− thresholds and refractive error is negative.

To quantify the strength of evidence that we observed of negative correlations, a Bayesian approach was applied[54,55] by using the BayesFactor package in R.[56] Bayes factors offer a nonbinary way of quantifying the subjective probability of a hypothesis. A larger Bayes factor indicates greater evidence for the hypothesis after the data are collected. The Bayes factor for the hypothesis that the S+ correlation was negative is 3.06; for S− a value of 1.75 was obtained. Labeling Bayes factor values defeats their purpose of continuously quantifying the evidence for the hypothesis, but Jeffreys[54] suggested 3 or larger could be referred to as "substantial" and 1 to 3 as "barely worth a mention." Others[57] have suggested the words "moderate" and "anecdotal" for these smaller Bayes factors. Thus, we have substantial evidence for a negative correlation between refractive error and S-cone increment thresholds, and weaker evidence for that same relationship with S-cone decrement thresholds.

Putting the question of statistical significance aside, the direction of the correlation of refractive error with S-cone blob thresholds is clearly more likely to be negative, as indicated by the bootstrap results and Bayes factor tests. Thus, higher S-cone thresholds (lower sensitivity) were associated with greater degrees of myopia. The negative correlations of refractive error and S-cone blob stimuli are consistent with a role for LCA in myopia development. In light of the work reviewed in the Introduction, these results provide at least tentative support for the hypothesis that reduced S-cone sensitivity in child development, persisting into adulthood, could cause the emmetropization mechanism(s) to be less able to use the blur at short wavelengths to regulate eye growth via the sign of defocus or via accommodation.

Before considering possible causes for a relationship between S-cone thresholds and refractive error in our study, two other possible mechanisms that could contribute to individual differences in myopia should be mentioned. The first is an LCA signal from the M- and L-cones. LCA varies continuously over the visible spectrum,[9,58] which produces differences in focal planes that are differentially detected by

Table 3. Pearson Correlation Coefficients Between Threshold and Refractive Error (Best Sphere) With Associated *P* Values and Bootstrap Confidence Intervals for *r*

Stimulus	*R*	*P*	*r*, 95% BCI
A Gabor	−0.03	0.85	−0.28, 0.25
L Gabor	−0.07	0.64	−0.33, 0.15
M Gabor	−0.03	0.49	−0.30, 0.15
S Gabor	0.10	0.167	−0.17, 0.37
S+ blob	−0.28	0.06	−0.50, −0.04
S− blob	−0.23	0.13	−0.46, 0.01

the L- and M-cones. But the differences in cone contrast induced by LCA between the L- and M-cones are relatively small compared to the differences between S-cones and the other cones. The lack of correlation between L- and M-cone detection thresholds and refractive error in our study might suggest that an M- versus L-cone LCA signal is not used by the emmetropization system. But given that we did not test L- and M-cones with the low frequency blobs used for S-cones, the hypothesis that the L- versus M-cone LCA signal can be used at low frequencies is currently untested.

Secondly, there is evidence that the emmetropization system is aided by high-intensity outdoor illumination.[59] Bright light stimulates intrinsically photosensitive retinal ganglion cells (iPRGCs), which are known to be involved in circadian rhythms and emmetropization.[60] iPRGCs are most sensitive to short wavelengths.[61] Our cone isolation procedures did not rule out stimulation of ipRGCs by our stimuli, and among our stimuli the nominally S-cone–isolating stimuli would produce the largest modulation of ipRGCs. However, ipRGCs are insensitive and slow,[62] absent from the fovea where our stimuli were placed,[63] and in general the role they play in functional vision is unclear. Thus, it seems very unlikely that ipRGCs contribute to the results of our study.

Our focus is on the potential relationships that we found between refractive error and S-cone thresholds. The causes of the individual differences in sensitivity of the S-cones could include differences in photopigment λ_{max}.[31] Another factor could be differences in magnitude of preretinal filtering by the lens and the macular pigment, both of which block short-wavelength light[24,64] and thereby decrease the S-cone adaptation level. Other potential sources of individual differences in S-cone sensitivity include genes involved in glucose metabolism.[53] However, these factors affect S-cone sensitivity without regard to the spatial characteristics of the stimulus, that is, they are not spatial frequency specific, which is not consistent with the lack of correlation of S-cone 3 cyc/deg Gabor sensitivity and refractive error found (Fig. 4; Table 2), whereas the effects of LCA are spatial frequency specific.

A possible interpretation of the difference in the results for the S-cone Gabors and the S-cone blob is as follows. S-cones are lacking in the central fovea[65,66] and S-cone density peaks in a ring at approximately 1° eccentricity.[67–69] However, there are individual differences in the mosaic of S-cones in the retina.[34,65,66] A spatial frequency of 3 cyc/deg, the frequency of the Gabors used in this experiment, is a relatively high frequency for S-cone detection.[51,52] Thus, the detection of the 3 cyc/deg S-cone Gabor stimulus is likely to be dependent upon sampling by the S-cones in the higher-density parafoveal S-cone ring.

S+ and S– blob increment and decrements are dominated by very low spatial frequencies and are likely to be detected by summing S-cone signals over a larger area around the central fovea.

This leads us to speculate that differences in observer S-cone mosaics may play a role in the control of myopia development. If myopes have fewer total S-cones in the central 3° to 4° of their retina, but a normal peak S-cone density in the parafoveal ring, then their ability to detect the S-cone blobs, but not S-cone Gabors, would be impaired as compared to emmetropes because of the lower spatial frequency of the blobs. Thus, if an LCA signal from short versus long wavelengths guides the emmetropization system via an integration of S-cone signals across a few central degrees of eccentricity, children with fewer total S-cones over the central retina may be predisposed to develop myopia. The same altered S-cone system that guides the emmetropization system toward myopia may be revealed by our detection task in adults.

Acknowledgments

Supported by Nation Institutes of Health grant EY0232-81 (FJR). The authors alone are responsible for the writing and content of the paper.

Disclosure: **C.P. Taylor**, None; **T.G. Shepard**, None; **F.J. Rucker**, None; **R.T. Eskew Jr**, None

References

1. Flitcroft D. The complex interactions of retinal, optical and environmental factors in myopia aetiology. *Prog Retin Eye Res*. 2012;31:622–660.
2. Vitale S, Cotch MF, Sperduto R, Ellwein L. Costs of refractive correction of distance vision impairment in the United States, 1999–2002. *Ophthalmology*. 2006;113:2163–2170.
3. Rein DB, Zhang P, Wirth KE, et al. The economic burden of major adult visual disorders in the United States. *Arch Ophthalmol*. 2006;124:1754–1760.
4. Frick KD. What the comprehensive economics of blindness and visual impairment can help us understand. *Indian J Ophthalmol*. 2012;60:406–410.
5. Wallman J, Winawer J. Homeostasis of eye growth and the question of myopia. *Neuron*. 2004;43:447–468.
6. Rucker FJ, Wallman J. Chick eyes compensate for chromatic simulations of hyperopic and myopic defocus: evidence that the eye uses longitudinal chromatic aberration to guide eye-growth. *Vis Res*. 2009;49:1775–1783.
7. Rucker FJ, Kruger PB. Accommodation responses to stimuli in cone contrast space. *Vis Res*. 2004;44:2931–2944.
8. Rucker F, Osorio D. The effects of longitudinal chromatic aberration and a shift in the peak of the middle-wavelength sensitive cone fundamental on cone contrast. *Vis Res*. 2008;48:1929–1939.
9. Atchison DA, Smith G. *Optics of the Human Eye*. Oxford: Butterworth Heinemann; 2000.
10. Foulds WS, Barathi VA, Luu CD. Progressive myopia or hyperopia can be induced in chicks and reversed by manipulation of the chromaticity of ambient light. *Invest Ophthalmol Vis Sci*. 2013;54:8004–8012.
11. Seidemann A, Schaeffel F. Effects of longitudinal chromatic aberration on accommodation and emmetropization. *Vis Res*. 2002;42:2409–2417.
12. Rucker FJ, Wallman J. Cone signals for spectacle-lens compensation: differential responses to short and long wavelengths. *Vis Res*. 2008;48:1980–1991.
13. Schaeffel F, Feldkaemper M. Animal models in myopia research. *Clin Exp Optom*. 2015;98:507–517.
14. Wisely CE, Sayed JA, Tamez H, et al. The chick eye in vision research: an excellent model for the study of ocular disease. *Prog Retin Eye Res*. 2017;61:72–97.
15. Osorio D, Vorobyev M, Jones C. Colour vision of domestic chicks. *J Exp Biol*. 1999;202:2951–2959.
16. Rucker F, Britton S, Spatcher M, Hanowsky S. Blue light protects against temporal frequency sensitive refractive changes. *Invest Ophthalmol Vis Sci*. 2015;56:6121–6131.
17. Rucker F, Henriksen M, Yanase T, Taylor C. The role of temporal contrast and blue light in emmetropization [published online ahead of print August 1, 2017]. *Vis Res*. doi:10.1016/j.visres.2017.07.003.
18. Kroger R, Wagner H-J. The eye of the blue acara (aequidens pulcher, cichlidae) grows to compensate for defocus due to chromatic aberration. *J Comp Physiol A*. 1996;179:837–842.
19. Jiang L, Zhang S, Schaeffel F, et al. Interactions of chromatic and lens-induced defocus during visual control of eye growth in guinea pigs (cavia porcellus). *Vis Res*. 2014;94:24–32.

20. Liu R, Qian Y-F, He JC, et al. Effects of different monochromatic lights on refractive development and eye growth in guinea pigs. *Exp Eye Res*. 2011;92:447–453.
21. Li X, Spiegel D, Bao J, Drobe B, Chen H. The effect of blue light on axial length changes induced by monocular optical defocus. In: *Abstracts of the 16th International Myopia Conference, IMC*. Birmingham, United Kingdom: Aston University; 2017:65.
22. Torii H, Kurihara T, Seko Y, et al. Violet light exposure can be a preventive strategy against myopia progression. *EBioMedicine*. 2017;15:210–219.
23. Roberts A, Zhu X, Wallman J. Lens-compensation under dim illumination: differential effects on choroidal thickness and ocular elongation. *Invest Ophthalmol Vis Sci*. 2003;44:1981–1981.
24. Stockman A, Sharpe LT. The spectral sensitivities of the middle-and long-wavelength-sensitive cones derived from measurements in observers of known genotype. *Vis Res*. 2000;40:1711–1737.
25. Stockman A, Sharpe LT, Fach C. The spectral sensitivity of the human short-wavelength sensitive cones derived from thresholds and color matches. *Vis Res*. 1999;39:2901–2927.
26. Kruger PB, Rucker FJ, Hu C, Rutman H, Schmidt NW, Roditis V. Accommodation with and without short-wavelength-sensitive cones and chromatic aberration. *Vis Res*. 2005;45:1265–1274.
27. Rucker FJ, Kruger PB. The role of short-wavelength sensitive cones and chromatic aberration in the response to stationary and step accommodation stimuli. *Vis Res*. 2004;44:197–208.
28. Rucker FJ, Kruger PB. Isolated short-wavelength sensitive cones can mediate a reflex accommodation response. *Vis Res*. 2001;41:911–922.
29. Ip JM, Saw S-M, Rose KA, et al. Role of near work in myopia: findings in a sample of Australian school children. *Invest Ophthalmol Vis Sci*. 2008;49:2903–2910.
30. Smith VC, Pokorny J. Chromatic-discrimination axes, CRT phosphor spectra, and individual variation in color vision. *J Opt Soc Am A Opt Image Sci Vis*. 1995;12:27–35.
31. Webster MA. Reanalysis of λ max variations in the stiles–burch 10 color matching functions. *J Opt Soc Am A*. 1992;9:1419–1421.
32. Stockman A, Sharpe L. Spectral sensitivity. In: Albright T, Masland R, eds. *The Senses: A Comprehensive Reference*. Vol 2. San Diego, CA: Academic Press Inc; 2008:87–100.
33. Deeb SS, Diller LC, Williams DR, Dacey DM. Interindividual and topographical variation of l: M cone ratios in monkey retinas. *J Opt Soc Am A Opt Image Sci Vis*. 2000;17:538–544.
34. Hofer H, Carroll J, Neitz J, Neitz M, Williams DR. Organization of the human trichromatic cone mosaic. *J Neurosci*. 2005;25:9669–9679.
35. Dacey DM, Packer OS. Colour coding in the primate retina: diverse cell types and cone-specific circuitry. *Curr Opin Neurobiol*. 2003;13:421–427.
36. Dacey DM, Crook JD, Packer OS. Distinct synaptic mechanisms create parallel s-on and s-off color opponent pathways in the primate retina. *Vis Neurosci*. 2014;31:139–151.
37. Webster M. Individual differences in color vision. In: *Handbook of Color Psychology*. Cambridge, UK: Cambridge University Press; 2015:197–215.
38. Pokorny J, Collins B, Howett G, Lakowski R, Lewis M. Procedures for testing color vision. In: *Technical Report, National Research Council Washington DC Committee on Vision*. Washington DC: Academic Press; 1981.
39. Estevez O, Spekreijse H. The silent substitution method in visual research. *Vis Res*. 1982;22:681–691.
40. Shepard TG, Swanson EA, McCarthy CL, Eskew RT Jr. A model of selective masking in chromatic detection. *J Vis*. 2016;16(9):3.
41. Chaparro A, Stromeyer CF III, Huang EP, Kronauer RE, Eskew RT Jr. Colour is what the eye sees best. *Nature*. 1993;361:348–350.
42. Wang Q, Richters DP, Eskew RT Jr. Noise masking of s-cone increments and decrements. *J Vis*. 2014;14(13):8.
43. Eskew R Jr, McLellan JS, Giulianini F. Chromatic detection and discrimination. In: Gegenfurtner K, Sharpe L, eds. *Color Vision: From Genes to Perception*. Cambridge, UK: Cambridge University; 1999:345–368.
44. Wetherill G, Levitt H. Sequential estimation of points on a psychometric function. *Br J Math Stat Psychol*. 1965;18:1–10.
45. Chen C-C, Foley JM, Brainard DH. Detection of chromoluminance patterns on chromoluminance pedestals I: threshold measurements. *Vis Res*. 2000;40:773–788.
46. Cole GR, Hine T, McIlhagga W. Detection mechanisms in l-, m-, and s-cone contrast space. *J Opt Soc Am A*. 1993;10:38–51.
47. Chambers J, Hastie T. *Statistical Methods*. Pacific Grove, CA: Wadsworth & Brooks/Cole; 1992:196–246.
48. Canty A, Ripley B. R Statistical Package Boot (2017). Available at: https://cran.r-project.org/package=boot. Accessed July 31, 2017.
49. Davison AC, Hinkley DV. *Bootstrap Methods and Their Application*. Vol 1. Cambridge, UK: Cambridge University Press; 1997.
50. Munafo MR, Nosek BA, Bishop DV, et al. A manifesto for reproducible science. *Nature Hum Behav*. 2017;1:0021.
51. Cavonius C, Estevez O. Contrast sensitivity of individual colour mechanisms of human vision. *J Physiol*. 1975;248:649–662.
52. Humanski RA, Wilson HR. Spatial frequency mechanisms with shortwavelength-sensitive cone inputs. *Vis Res*. 1992;32:549–560.
53. Bosten JM, Bargary G, Goodbourn PT, Hogg RE, Lawrance-Owen AJ, Mollon J. Individual differences provide psychophysical evidence for separate on-and off-pathways deriving from short-wave cones. *J Opt Soc Am A Opt Image Sci Vis*. 2014;31:A47–A54.
54. Jeffreys H. *Theory of Probability*. Oxford: Oxford University Press; 1961.
55. Ly A, Verhagen J, Wagenmakers E-J. Harold Jeffreys's default Bayes factor hypothesis tests: explanation, extension, and application in psychology. *J Math Psychol*. 2016;72:19–32.
56. Morey RD, Rouder JN. BayesFactor: Computation of Bayes Factors for Common Designs, 2018. R Package Version 0.9.12-4.2. Available at: https://CRAN.R-project.org/package=BayesFactor. Accessed May 20, 2018.
57. Wetzels R, Wagenmakers E-J. A default Bayesian hypothesis test for correlations and partial correlations. *Psychon Bull Rev*. 2012;19:1057–1064.
58. Thibos LN, Ye M, Zhang X, Bradley A. The chromatic eye: a new reduced-eye model of ocular chromatic aberration in humans. *Appl Opt*. 1992;31:3594–3600.
59. Norton TT, Siegwart JT Jr. Light levels, refractive development, and myopia–a speculative review. *Exp Eye Res*. 2013;114:48–57.
60. Phillips JR, Backhouse S, Collins AV. Myopia, light and circadian rhythms. In: Rumelt S, ed. *Advances in Ophthalmology*. London, UK: InTech; 2012.
61. Bailes HJ, Lucas RJ. Human melanopsin forms a pigment maximally sensitive to blue light (λmax 479 nm) supporting activation of gq/11 and gi/o signalling cascades. *Proc Royal Soc B*. 2013;280:20122987.
62. Zele AJ, Feigl B, Adhikari P, Maynard ML, Cao D. Melanopsin photoreception contributes to human visual detection, temporal and colour processing. *Sci Rep*. 2018;8:3842.

63. Nasir-Ahmad S, Lee S, Martin PR, Grünert U. Melanopsin-expressing ganglion cells in human retina: morphology, distribution, and synaptic connections [published online ahead of print January 18, 2017]. *J Comp Neurol*. doi:10.1002/cne.24176.
64. Stockman A, Jagle H, Pirzer M, Sharpe LT. The dependence of luminous efficiency on chromatic adaptation. *J Vis*. 2008; 8(16):1.
65. Williams DR, MacLeod DI, Hayhoe MM. Punctate sensitivity of the blue-sensitive mechanism. *Vis Res*. 1981;21:1357–1375.
66. Williams DR, MacLeod DI, Hayhoe MM. Foveal tritanopia. *Vis Res*. 1981;21:1341–1356.
67. Curcio CA, Allen KA, Sloan KR, et al. Distribution and morphology of human cone photoreceptors stained with anti-blue opsin. *J Comp Neurol*. 1991;312:610–624.
68. Curcio CA, Hendrickson AE. Organization and development of the primate photoreceptor mosaic. *Prog Retin Res*. 1991; 10:89–120.
69. Ahnelt PK, Kolb H. The mammalian photoreceptor mosaic-adaptive design. *Prog Retin Eye Res*. 2000;19:711–777.